Biaxial Mechanical Properties of Human Ureter under Tension

Aisa Rassoli,[1] Mohammad Shafigh,[2] Amirsaeed Seddighi,[3] Afsoun Seddighi,[3] Hamidreza Daneshparvar,[4] Nasser Fatouraee [1]

[1] *Biological Fluid Mechanics Research Laboratory, Biomedical Engineering Faculty, Amirkabir University of Technology (Tehran Polytechnic), Tehran, Iran.*
[2] *Department of Engineering, Islamshahr Branch, Islamic Azad University, Tehran, Iran.*
[3] *Functional Neurosurgery Research Centre, Shohada Tajrish Hospital, Shahid Beheshti University of Medical Sciences, Tehran, Iran.*
[4] *Legal Medicine Research Center, Legal Medicine Organization, Tehran, Iran.*

Corresponding Author:

Nasser Fatouraee, Ph.D
Biological Fluid Mechanics Research Laboratory, Biomedical Engineering Faculty, Amirkabir University of Technology (Tehran Polytechnic), Tehran, Iran.

Tel: +98 21 6454 2368
Fax: +98 21 6646 8186
E-mail: Nasser@aut.ac.ir

Purpose: The Mechanical properties of the ureteral wall may be altered by certain diseases such as megaureter. Ureter compliance and wall tension alterations can occur, leading to some abnormalities such as reflex mechanisms. Familiarizing with the mechanical properties of the ureter can help us advance in the understanding of urinary tract diseases.

Materials and Methods: A constitutive model that can predict the mechanical response of ureteral tissue under complex mechanical loading is required. Parameters characterizing the mechanical behaviour of the material were estimated from planar biaxial test data, where human ureter specimens were simultaneously loaded along the longitudinal and circumferential directions.

Results: The biaxial stress-stretch curve was plotted and fitted to a hyperelastic four-parameter Fung type model and five-parameter Mooney-Rivlin model. The average strength in the longitudinal direction was 3.48 ± 0.47 MPa and 2.31 ± 0.46 MPa ($P < .05$) for the circumferential direction.In the Fung model the value of parameter a_2 (0.699 ± 0.17) was higher than a_1 (0.279 ± 0.07), which may be due to the collagen fiber orientation's preference along the longitudinal axis.

Conclusion: According to this study, it seems that ureter tissue is stiffer in the longitudinal than in the circumferential direction and maybe the collagen fiber are along the axial axes. Also the specimens showed some degree of anisotropy.

Keywords: biomechanical phenomena; computer simulation; elasticity; ureter; physiology; models; biological; peristalsis; stress; mechanical.

INTRODUCTION

Ureters are tubes that are made up of smooth muscle fibres, and their function is to transfer urine from the kidneys to the bladder.[1] In the adult, the ureter is usually 25-30 cm long and about 3-4 mm in diameter.[2-4] Histologically, the ureter contains the muscle cover that causes the transmission of urine from the kidney to the bladder and alters its flexibility. Megaureter is one of the most important abnormalities of the upper urinary tract,[5-9] which is classified by some urologists into those attributable to: reflux, obstruction, unrelated to reflux and unrelated to obstruction. A quantitative analysis characterizing peristaltic flow will further expand our knowledge of the ureter and also assist in the design of flow-aided devices to correct some abnormalities. The anatomical complexity of the ureter has considerable clinical importance, therefore, models that contain mechanical properties of the ureteral wall with actual modelling of peristaltic flow can yield applied results with accurate interpretations. Hence, a constitutive model that can reliably predict the mechanical behaviour of the ureteral tissue is necessary.

Notwithstanding the physiological and clinical relationship of ureteral elasticity, insufficient data is available about the mechanical behaviour of ureteral wall. Among the few studies, Yin and Fung performed uniaxial tensile tests on ureter from a variety of mammals and human foetus. Important findings were that ureters exhibit an anisotropic, nonlinear and pseudo-elastic behaviour over finite strain, and that their behaviour differs with the region under strain.[10] Sokolis investigated the biaxial properties of rabbit ureter by applying internal pressure through inflation and used the four-parameter Fung-type SEF model to describe them.[11] Although the uniaxial tensile test data were presented comprehensively they were not sufficient to determine mechanical properties like nonlinear and anisotropic responses. Moreover, the inflation tests lacked the adaptability of a planar test, in addition to the fact that the sample sizes in these tests were dependent on the pressure and size of the nozzle.[12] To the authors' knowledge, experimental measurements obtained from the biaxial planar loading have so far not been considered in the development of constitutive models for the ureter.

Hence, the goal of this study was to develop an anisotropic constitutive model for the ureter wall. Planar biaxial tests were performed on specimens by loadings applied along the circumferential and longitudinal directions. Then, the data of the experimental tests were modelled by the anisotropic four-parameter Fung-type model and the anisotropic modified Mooney-Rivlin Model.

MATERIALS AND METHODS

Sample Preparation

Human ureter was used in this study. Before resecting the samples, written consent was obtained from the families of the deceased. They were asked to sign the consent form prepared by the Legal Medicine Organization. Eighteen ureter specimens were used in this study, extracted from 9 healthy upper urinary tracts. To protect the samples from dehydration, tissues were cleaned and stored in physiological saline 0.9%. The tests were performed within 10 hours after extraction. Thickness measurements were taken from different regions of the samples by using a micrometre. Out of necessity, the mean thickness was utilized for stress calculations. The central parts of the specimens were cut into segments, then cut along the longitudinal axis, and splayed to obtain square 6×6 mm^2 samples for biaxial testing. During the test, the samples were stored in 0.9% physiological saline heated by a heater to 37°C.

Testing Protocol

Device description: Tests on each specimen were done by the planar biaxial testing system with strain controlled capability. The clamps of this system were able to directly hold samples with dimensions of $\geq 5 \times 5$ mm^2 without damaging the tissue (Figure 1). In order to preserve the mechanical properties, samples were kept wet at a temperature of 37°C by using a temperature controlled water bath. Tensile forces were measured by two UMAA 2 kilogram-force (kgf) load cells (Dacell Co., Ltd, Korea Corporation, Korea). The required tensile forces, in this device, were applied by four micro stepper motors with a resolution of 0.36 degrees and with a nominal torque of 1.2 kg/cm (Autonics Corporation, Gyeonggi-do, Korea). Four drivers were used to drive the stepper motors (Autonics model MD5-H14). To measure the tissue deformation, an Universal Serial Bus (USB) digital microscope camera was used (300 × zoom, 30 Hz and reso-

lution of 480 × 640). Data sent by the controller were transferred to a computer and saved there. To synchronize the data, load cells and camera data were simultaneously saved at a frequency of 5 Hertz (Hz).

Loading protocols: After each specimen was placed on the testing system, a preload of 0.01 Newton (*N*) was applied along both axes to obtain meaningful measurements. A low loading rate was considered for a quasi-static test by selecting the strain rate at 0.02 mm/s for all tests. Force and displacement data were recorded at 0.2 second intervals (frequency of 5 Hz).The digital microscope camera's data were processed with the ImageJ package to obtain stretch in each direction. We could not use ink markers in stretch (displacement) measurement, because of the small dimensions of the samples. The Initial distance between the ends of each clamp was considered as the reference measure for sample length in both directions.

The stress-strain curve for each specimen was obtained in two axes [the (11) axes corresponding to the circumferential direction and the (22) axes corresponding to the longitudinal direction].The experimental stresses for the samples were computed as follows:

$$\sigma_{11}^{exp} = \lambda_1 \frac{F_{11}}{l_2 t}$$

(1)

$$\sigma_{22}^{exp} = \lambda_2 \frac{F_{22}}{l_1 t}$$

(2)

where $\lambda 1$ and $\lambda 2$ are the stretch ratios, F11 and F22 are the forces measured by the load cells, t is the thickness of the samples, and l_1 and l_2 are the unloaded widths of the samples in the two directions. the unloaded widths of the samples in the two directions.

Constitutive Model Development

In this study, ureter was modeled as an incompressible, homogeneous and hyperelastic material. These assumptions justify the existence of a strain energy function W which is the criterion for the stored energy in the materials as a result of the deformation. With the use of strain energy function, the stresses can be computed from the strains as follows:

$$\sigma_{ij} = PI + 2F_{ij}\frac{\partial w}{\partial C_{ij}}F_{ij}^T = pI + F_{ij}\frac{\partial w}{\partial E_{ij}}F_{ij}^T$$

(3)

where σij is the Cauchy stress tensor, P is the Lagrange multiplier introduced to enforce incompressibility, $C_{ij} = F_{ij}^T F_{ij}$ is the right Cauchy–Green deformation tensor, $E_{ij} = 0.5(C_{ij}-I_{ij})$ is the Green–Lagrange strain tensor, I_{ij} is the identity unit tensor and F_{ij} is the deformation gradient tensor which can be described as F= ∂x/∂x' in which x' and x are the positions of material points in the reference and current configuration, respectively. Note that in this study the shear strains were negligible and hence ignored in the subsequent data analysis.

Based on the strain energy function and hyperelastic models,[16-20] two appropriate constitutive models were chosen to express the mechanical properties of the ureter; as these models have been used previously for other soft tissues.

The first model utilized was a Fung-type model[16] able to describe the anisotropic behaviour of tissue. In the Fung model, the strain energy density is given by:

$$w(Q) = \frac{1}{2}c(e^Q - 1)$$

(4)

where $Q(E) = a_1 E_{11}{}^2 + a_2 E_{22}{}^2 + 2a_3 E_{11}E_{22}$, and c ,a_1, a_2 and a_3 are constitutive parameters.

The Cauchy stress components in the two directions were then calculated as follows:

The second model was the modified Mooney-Rivlin model

$$\sigma_{11} = \left\{ \frac{1}{2}c\lambda_1^2[a_1(\lambda_1^2 - 1) + a_3(\lambda_2^2 - 1)] * e^{\frac{1}{4}[a_1(\lambda_1^2-1)^2 + a_2(\lambda_2^2-1)^2 + 2a_3(\lambda_1^2-1)(\lambda_2^2-1))} \right\}$$

(5)

$$\sigma_{22} = \left\{ \frac{1}{2}c\lambda_2^2[a_2(\lambda_2^2 - 1) + a_3(\lambda_1^2 - 1)] * e^{\frac{1}{4}[a_1(\lambda_1^2-1)^2 + a_2(\lambda_2^2-1)^2 + 2a_3(\lambda_1^2-1)(\lambda_2^2-1))} \right\}$$

(6)

which shows the anisotropic behaviour of the tissues and can also be implemented in many standard FE packages. The strain energy density function of this model is given by:

$$w = C_1(I_1 - 3) + D_1[\exp(D_2(I_1 - 3)) - 1] + \frac{k_1}{2k_2}[\exp[k_2(I_4 - 1)^2 - 1])$$

(7)

are the model parameters[21].

According to the strain energy function, Cauchy stresses in the two axes are as follows:
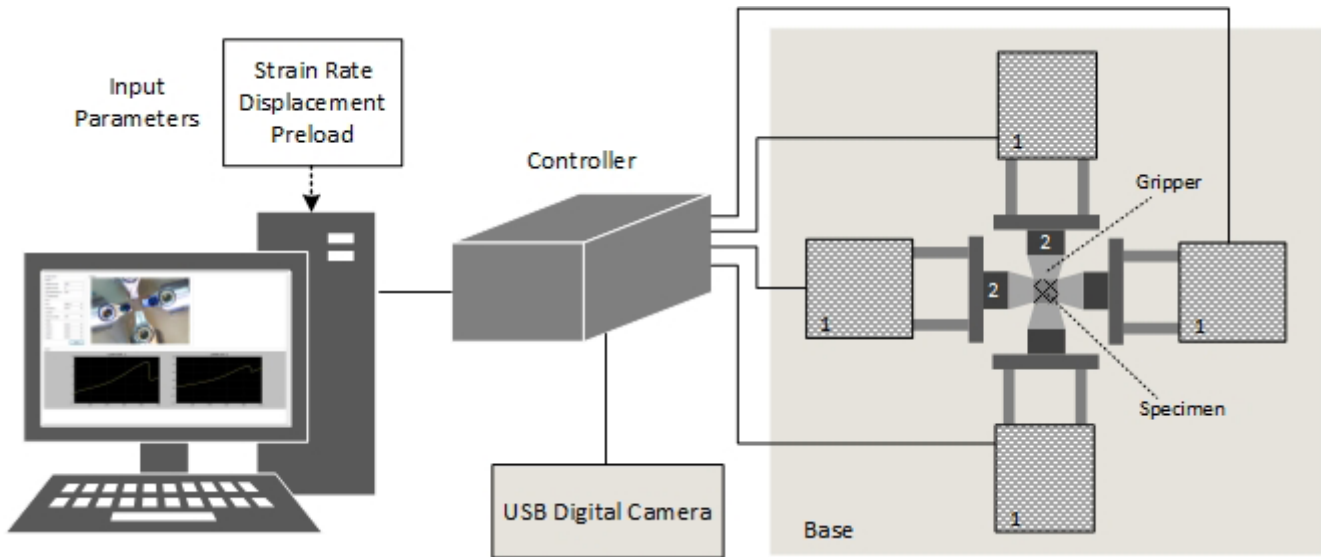
Figure 1. Diagram of the biaxial tensile test system (1: the micro stepper motors; 2: the load cells)

$$\sigma_{11} = \left(2 \times (\lambda_1^2 - \lambda_3^2)(C_1 + D_1 \times D_2 \times \exp(\lambda_1^2 + \lambda_2^2 + \lambda_3^2 - 3))\right) + \cdots$$
$$(2 \times k_1 \times \lambda_1^2 \times (\lambda_1^2 - 1) \exp\left(k_2 \times (\lambda_1^2 - 1)^2\right))$$

(8)

$$\sigma_{22} = \left(2 \times (\lambda_2^2 - \lambda_3^2)(C_1 + D_1 \times D_2 \times \exp(\lambda_1^2 + \lambda_2^2 + \lambda_3^2 - 3))\right)$$

(9)

Experimental data were then fitted to Cauchy stress of each model by using genetic algorithm and the parameters of constitutive models were obtained for each data set. For the Fung model, anisotropy was also calculated as follows:

$$\text{Anisotropy} = \min\left[\frac{a_1 + a_3}{a_2 + a_3}, \frac{a_2 + a_3}{a_1 + a_3}\right]$$

(10)

Statistics
The results of the experimental tests and constitutive models are presented as average ± SD. The two-tailed paired t-test was used to compare the longitudinal and circumferential directions stiffness with statistical package for the social science (SPSS Inc, Chicago, Illinois, USA) version 22.0. Significance was set at *P < .05*

RESULTS
Since some of the specimens were unsuitable for testing (some specimens were very soft or they had degenerated during the tests), ten samples were appropriate for the biaxial tests. Figure 2 shows the Cauchy stress-stretch curves obtained from the biaxial mechanical testing of all specimens in the circumferential (1-a) and in the axial (1-b) directions. It cannot be said that the axial direction was consistently the stiffer (or less stiff) direction. But on average, the specimens acted stiffer in the axial direction than in the circumferential direction. Simultaneous loading in these two orthogonal directions also allowed us to conclude that the mechanical response in one direction was influenced by the characteristics of the other direction. Then, these Cauchy stress-stretch curves were fitted to the Fung and modified Mooney-Rivlin constitutive equations through Eqs.[5,6,8,9] Table represents the Fung and Mooney-Rivlin best-fit material parameters for all the existing data. the mean values calculated are presented in the last column. Based on the calculated RMS error (Table), the Mooney-Rivlin model approximately provides the best qualitative fit to the data.

By using these material constants, stretch-stress curves were extracted and plotted in Figure 3. The mean biaxial stretch-stress curve for ureter was also obtained from the average Fung constants mentioned in Table and plotted in Figure 2 as well. To validate the fitting method, the experimental data and model curves obtained from the material constants were illustrated together in Figures 4 and 5 for specimens. It can be seen that predicted models are in agreement with experimental data.
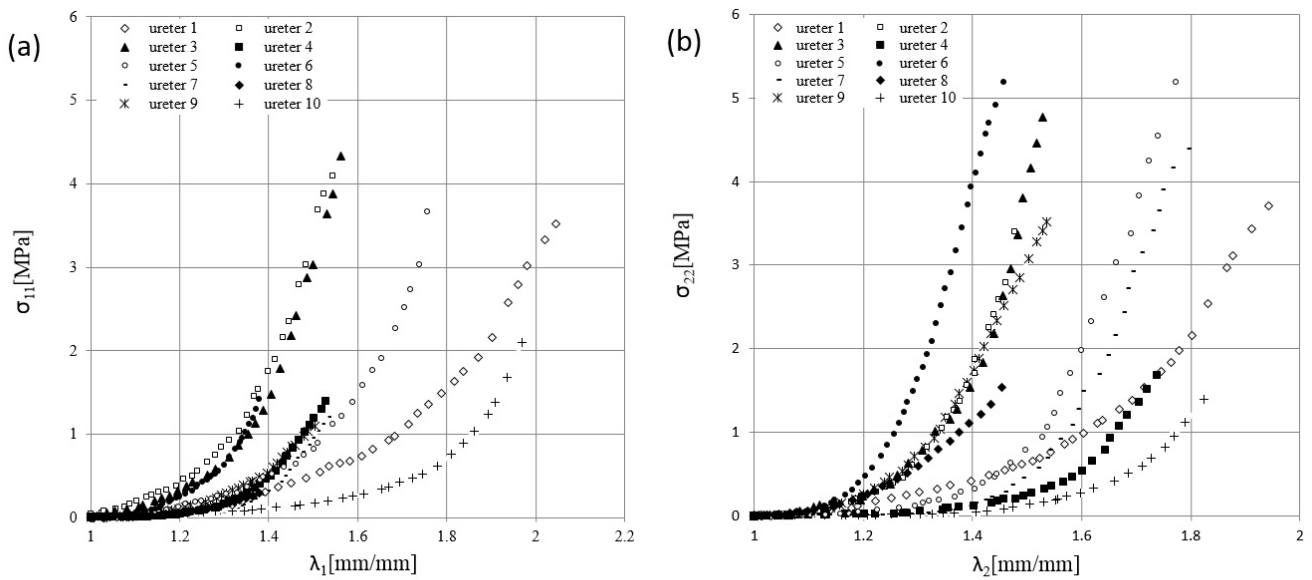
Figure 2. Stress-stretch data for human ureter. The left hand plots (a) show the stresses and stretches in the circumferential (11) direction while the right hand plots (b) show the stresses and stretches in the longitudinal (22) direction.

DISCUSSION

This study provides a complete set of experimental planar biaxial data for human ureter fitted to the two anisotropic constitutive models to describe its mechanical characteristics. The reliance of the constitutive behavior on the specific position in the tissue was overlooked and a homogeneous response was presumed. This approach, although suitable for modelling the behavior of the ureteral tissue at the macroscopic level, cannot associate the observation made with the naked eye with the microstructure. The soft tissue walls include extracellular matrix proteins and cells, which give origin to a multi-layered composite material where each layer has specific composition, organization and mechanical property.

Stiffer behaviour in the longitudinal direction had been reported in earlier research on uniaxial tensile tests for dog ureter as well.[10] Inflation tests on rabbit ureter[11] also showed stiffer characteristics in the axial direction. In this
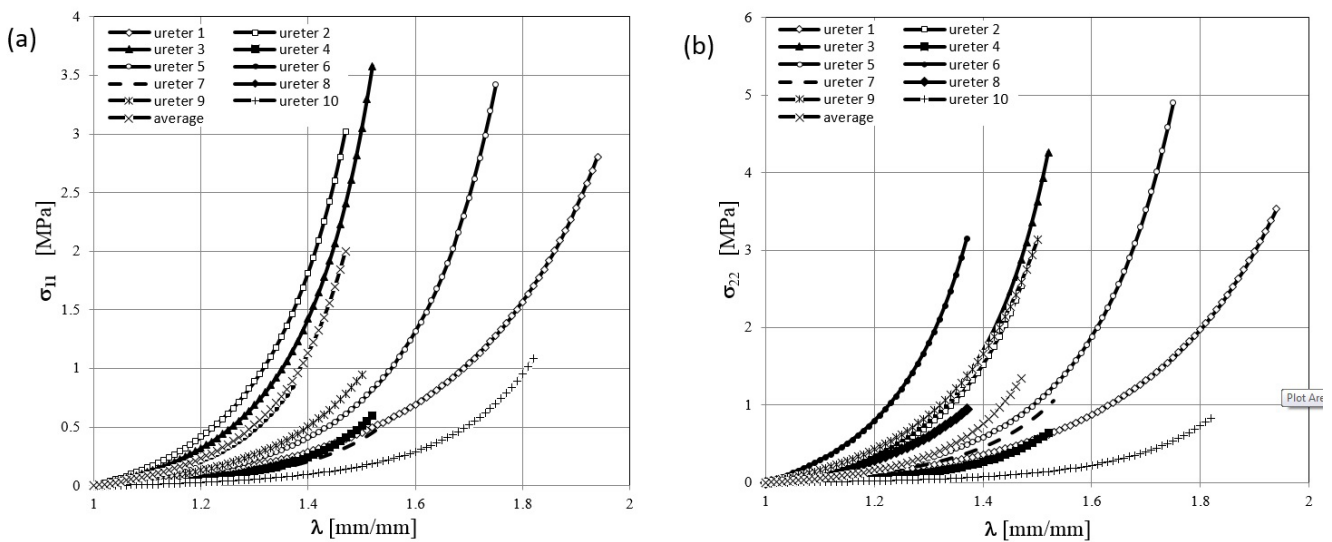
Figure 3. Stress-stretch curves obtained from the Fung constants in circumferential (a) and axial (b) directions ($\lambda_1 = \lambda_2 = \lambda$).
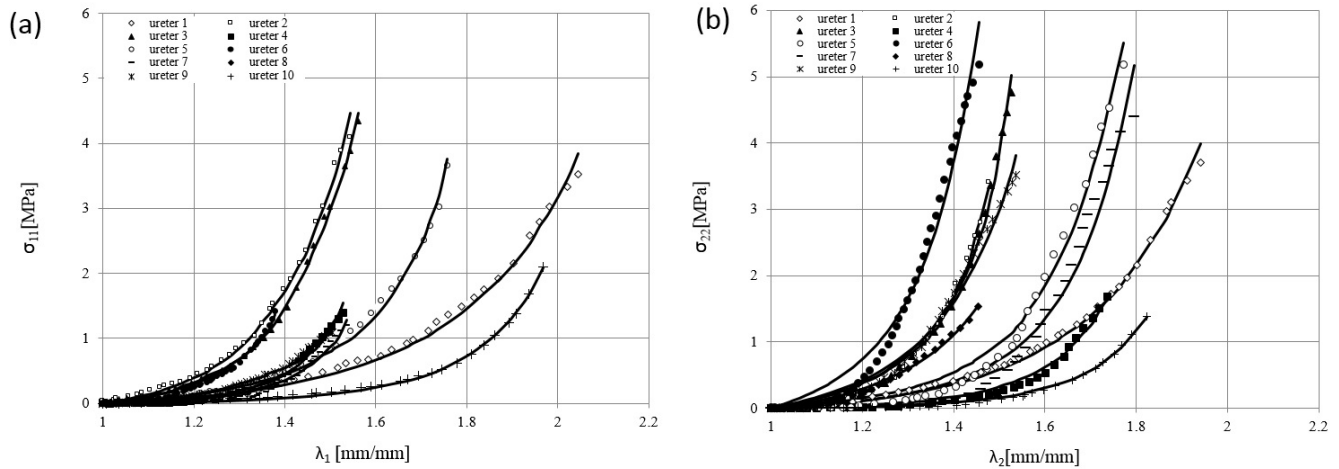
Figure 4. Comparison of stretch-stress curves of Fung model and experimental data for all specimens in circumferential (a) and axial (b) directions.

study, samples showed maximum stiffness in the longitudinal direction. The average strength in the longitudinal direction was 3.48 ± 0.47 MPa and 2.31 ± 0.46 MPa $P < .05$ for the circumferential direction. The behavior of the Soft tissue up to the rupture point in the longitudinal and circumferential direction depends on the exposure of collagen, elastin fiber network and smooth muscle cells in its different layers. Elastin fibers are involved in the initial phase of stretching; then, collagen fibers also participate in stress tolerance. The higher stiffness of the ureteral tissue in the longitudinal direction than in the circumferential direction indicates that the collagen is more effective in this direction because the

elastin fibers have low strength.[22] Under high strain ratio, the role of collagen is more important than that of elastin. The current investigation's limitation is its method of sample preparation, as it was not possible for us to do the experiments when the tissues were alive. So we cannot discuss the small muscle cells' roles in the mechanical properties of the ureteral tissue because when the tissue is alive, smooth muscle cells and their tension also contribute to the development of overall wall tension.

As aforementioned we chose two anisotropic constitutive models for our biaxial data, where both models are well established as soft tissue materials and widely cited within
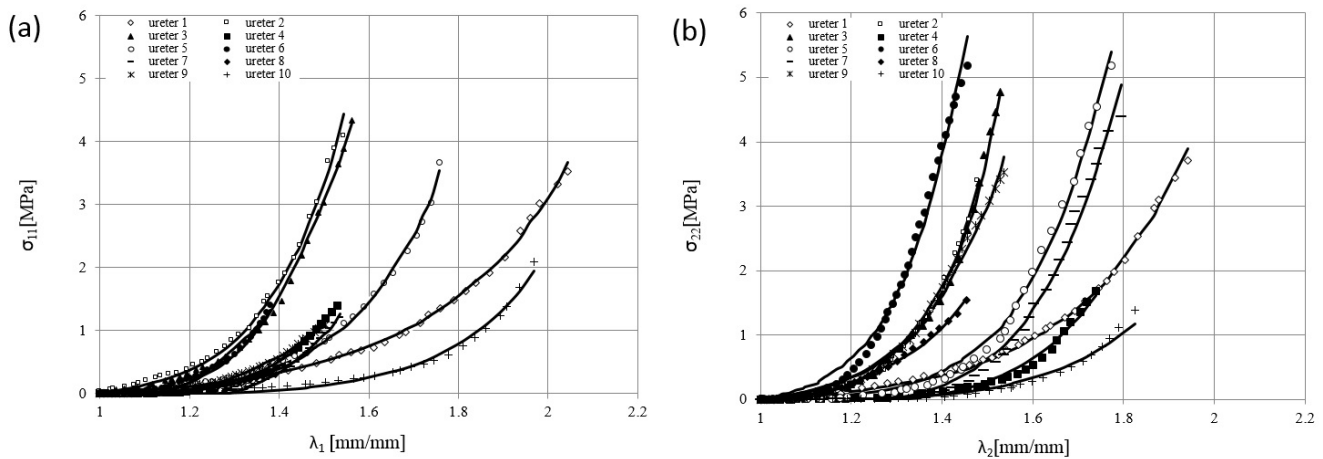
Figure 5. Comparison of stretch-stress curves of Mooney-Rivlin model and experimental data for all specimens in circumferential (a) and axial (b) directions.

Fung	C (MPa)	a1	a2	a3	Anisotropy	RMS (MPa)
Ureter 1	1.8955	0.1202	0.1590	0.0291	0.79	0.0165
Ureter 2	1.0372	0.7139	0.5293	0.4299	0.84	0.0237
Ureter 3	0.8891	0.5528	0.7477	0.4663	0.84	0.0244
Ureter 4	0.1632	0.1383	0.2221	0.8551	0.92	0.0106
Ureter 5	0.7525	0.2138	0.4090	0.2356	0.69	0.0291
Ureter 6	0.9477	0.1944	1.8774	0.4231	0.27	0.0349
Ureter 7	0.3262	0.3556	0.9223	0.1229	0.46	0.0331
Ureter 8	0.6828	0.1432	1.1083	0.1471	0.23	0.0073
Ureter 9	1.1357	0.0671	0.8423	0.2702	0.3	0.0215
Ureter 10	0.1631	0.2947	0.1743	0.2203	0.77	0.0053
Average	0.4056	0.7091	0.1856	0.8892	0.67	0.0083
Mooney-Rivlin	C_1 (MPa)	D_1 (MPa)	D_2	k_1 (MPa)	k_2	RMS (MPa)
Ureter 1	0.0395	0.2223	0.3566	-0.0100	0.1058	0.0109
Ureter 2	0.0203	0.1820	0.8502	0.0430	0.4023	0.0205
Ureter 3	-0.7233	1.3778	0.4801	-0.0558	0.3676	0.0244
Ureter 4	-0.2411	0.2714	0.4694	0.0515	0.1970	0.0091
Ureter 5	-0.1136	0.2302	0.5595	-0.0276	0.3615	0.0204
Ureter 6	-0.1082	0.7183	0.7736	-0.4032	0.9814	0.0255
Ureter 7	-0.4796	0.5492	0.4839	-0.0559	0.7150	0.0185
Ureter 8	-0.1623	0.4968	0.5679	-0.1416	0.8185	0.0046
Ureter 9	-0.3702	1.1924	0.4526	-0.2232	0.4047	0.0154
Ureter 10	-0.0754	0.1529	0.3494	0.0031	0.2423	0.012
Average	-0.1114	0.2050	0.6803	0.0402	0.9106	0.0039

the pertinent literature. The Fung-type exponential model has been used to describe the mechanical properties of arteries,[16] but it has also been applied for myocardium,[23] epicardium,[24] rabbit ureter[11] and porcine intestine.[25] The Mooney-Rivlin model formulations based on polynomials and exponentials of strain invariants are also common in the literature[26,27] and have been implemented in many standard FE packages. These constitutive models demonstrated mechanical anisotropy and nonlinearity of the tissues, and the data (Table) present some degree of anisotropy for ureteral wall.

As mentioned, on average, the specimens acted stiffer in the longitudinal direction than in the axial direction. In the Fung model the value of parameter a_2 (0.699 ± 0.17) was higher than a_1 (0.279 ± 0.07), which may be due to the collagen fiber orientation's preference along the longitudinal axis, as earlier justified by the extracellular matrix component of ureteral tissue.[11]

All of the models presented in this study were nonlinear and anisotropic. In particular, the Mooney-Rivlin model is an anisotropic model which can be used for fluid-structure interaction (FSI) numerical analysis in finite element analyses (FEA) packages (e.g. a FSI procedure in a commercial finite-element package named ADINA). Although the two models considered in this paper are phenomenological, they may be helpful as research references, offering good descriptive capabilities.

More research is required to determine the efficacy of small muscle cells on the mechanical properties of the ureter through in-vivo experiments. Moreover, further experimental investigations are needed to compare the mechanical properties of different segments of the ureter using the planar biaxial tensile test, and to compare the strength of the left and right ureteral tissues.

CONCLUSION

In this study the mechanical properties of human ureter have been determined by using a biaxial mechanical device. The resultant stretch-stress curves from the experimental data

were fitted to the four-parameter Fung-type model as well as the modified Mooney-Rivlin model, and the anisotropy values of the samples were calculated by the constitutive Fung model parameters. The samples showed some degree of anisotropy. The curves, on average, also showed stiffer behaviour in the longitudinal direction than in the circumferential direction. To conclude, this study may be used as a reference for the numerical simulation of ureter.

ACKNOWLEDGEMENTS

ETHICAL STANDARDS

As mentioned earlier in the methods section, the human samples used in this study were taken from cadavers preserved in the Iranian Legal Medicine Organization. The families of the deceased had given their informed consent prior to resection. Moreover, authorization to use these specimens was granted by the Iranian Legal Medicine Organization to the research team under letter no. p/49751, dated 11/08/2013. Therefore, the standards laid down in the Declaration of Helsinki have been adhered to.

AUTHORS' CONTRIBUTION

Rasooli contributed to the modeling, data analysis, and manuscript writing. She also performed the experiments. Shafigh helped with the experiments, specimen acquiring, and manuscript writing. Seddighi acted as the consultant in the medical aspects of the project and helped evaluate the results. Daneshparvar collaborated with the group from the Legal Medicine Organization and was responsible for all the procedures up to resection. And Fatouraee supervised the project through protocol development and manuscript editing. All authors read and approved the final manuscript.

CONFLICT OF INTEREST

None declared.

REFERENCES

1. Vahidi B, Fatouraee N, Imanparast A, Nasiraei-Moghaddam A. A mathematical simulation of ureter:effect of the model parameters on ureteral pressure/flow relations. J Biomech Eng. 2011;133:1-9.

2. Jimenez Lozano JN. Peristaltic flow with application to ureteral biomechanics. Ph.D. Thesis in Mechanical Engineering, Notre Dame University, Indiana, USA;2009 .

3. Woodburne RT, Lapides J. The ureteral lumen during peristalsis. Am J Anat. 1972;133:225-8.

4. Walsh PC, Wein AJ, Kavoussi LR, Peters CA, Novick AC. Campbell's Urology. (4 Volume Set), 8th Edition, Elsevier Science;2002.

5. Smith ED, Cussen LJ, Glenn J, et al. Report of working party to establish an international nomenclature for the large ureter. Birth Def. 1977;13:3-8.

6. Shokeir AA, Nijman RJM. Primary megaureter:current trends in diagnosis and treatment. BJU Int. 2000;86:861-8.

7. Keating MA, Escala J, Snyder 3rd H M, Heyman S, Duckett JW. Changing concepts in management of primary obstructive megaureter. J Urol. 1989;142(2 Pt 2):636-40.

8. Biserte J. Surgical treatment of primary mega-ureter. J Prog Urol. 1997;7:112-9.

9. King LR. Megaloureter: definition, diagnosis and management. J Urol. 1980;123:222-3.

10. Yin FCP, Fung YC. Mechanical properties of isolated mammalian ureteral segments. AM J Physiol. 1971;221:1484-93.

11. Sokolis DP. Multiaxial mechanical behavior of the passive ureteral wall: experimental study and mathematical characterization. Comput Methods Biomech Biomed Engin. 2012;15:1145-56.

12. Hung H, Chong C, Steinhart A, Trexler J, Billiar K. Design of a biaxial test device for compliant tissue. Bioengineering Conference. Proceedings of the IEEE 31st Annual Northeast. 2005;April;200-201.

13. Sun W, Sacks MS, Scott MJ. Numerical simulations of the planar biaxial mechanical behavior of biological materials. ASME Summer Bioengineering, Miami, FL. 2003.

14. Humphrey JD, Strumpf RK, Yin FCP. Determination of a constitutive relation for passive myocardium: A New Functional Form. J Biomech Eng. 1990;112:333-9.

15. Humphrey JD, Strumpf RK, Yin FCP. Determination of a constitutive relation for passive myocardium: II. Parameter Estimation. J Biomech Eng. 1990;112:340-6.

16. Fung YC, Fronek K, Patitucci P. Pseudoelasticity of arteries and the choice of its mathematical expression. AM J Physiol. 1979;237:620-31.

17. Holzapfel GA, Gasser TC, Ogden RW. A new constitutive framework for arterial wall mechanics and a comparative study of material models. J Elasticity. 2000;61:1-48.

18. Holzapfel GA, Eberlein R, Wriggers P, Weizsacker H. Large strain analysis of soft biological membranes: Formulation and finite element analysis. Comput Method APPL M. 1996;132:45-61.

19. Holzapfel GA, Gasser TC, Ogden RW. Comparison of a multi-layer structural model for arterial walls with a Fung-type model, and issues of material stability. J Biomech Eng. 2004;126:264-75.

20.   Holzapfel GA. Similarities between soft biological tissues and rubberlike materials. In constitutive models for rubber-proceedings, Balkema. 2005;4:607.

21.   Yang C, Bach RG, Zheng J, et al. In vivo IVUS-based 3-D fluid-structure interaction models with cyclic bending and anisotropic vessel properties for human atherosclerotic coronary plaque mechanical analysis. IEEE Trans Bio Med Eng. 2009;56:2420-8.

22.   Sokolis DP, Kefaloyannis EM, Kouloukoussa M, Marinos E, Boudoulas H, Karayannacos PE. A structural basis for the aortic stress–strain relation in uniaxial tension. J Biomech. 2006;39:1651-62.

23.   Yin FC, Strumpf RK, Chew PH, Zeger SL. Quantification of the mechanical properties of noncontracting canine myocardium under simultaneous biaxial loading. J Biomech. 1987;20:577-89.

24.   Humphrey JD, Strumpf RK, Yin FCP. A constitutive theory for biomembranes: application to epicardial mechanics. J Biomech Eng.1992;114:461-6.

25.   Bellini C, Glass P, Sitti M, Di Martino ES. Biaxial mechanical modeling of the small intestine. J Mech Behav Biomed. 2011;4:1727-40.

26.   Kural MH, Cai M, Tang D, Gwyther T, Zheng J, Billiar KL. Planar biaxial characterization of diseased human coronary and carotid arteries for computational modeling. J Biomech. 2012;45:790-8.

27.   Tang D, Yang C, Kobayashi S, et al. 3D MRI-based anisotropic FSI models with cyclic bending for human coronary atherosclerotic plaque mechanical analysis. J Biomech Eng. 2009;131:061010.